MOLECULAR AND CELLULAR BIOLOGY, Mar. 1997, p. 1144–1151 Vol. 17, No. 3
0270-7306/97/$04.00+0

The Decline in Human *Alu* Retroposition Was Accompanied by an Asymmetric Decrease in SRP9/14 Binding to Dimeric *Alu* RNA and Increased Expression of Small Cytoplasmic *Alu* RNA

JASMIT SARROWA, DAU-YIN CHANG, AND RICHARD J. MARAIA*

Laboratory of Molecular Growth Regulation, National Institute of Child Health and Human Development, National Institutes of Health, Bethesda, Maryland 20892

Received 18 October 1996/Accepted 26 November 1996

***Alu* interspersed elements are inserted into the genome by a retroposition process that occurs via dimeric *Alu* RNA and causes genetic disorders in humans. *Alu* RNA is labile and can be diverted to a stable left monomer transcript known as small cytoplasmic *Alu* (sc*Alu*) RNA by RNA 3′ processing, although the relationship between *Alu* RNA stability, sc*Alu* RNA production, and retroposition has been unknown. In vivo, *Alu* and sc*Alu* transcripts interact with the *Alu* RNA-binding subunit of signal recognition particle (SRP) known as SRP9/14. We examined RNAs corresponding to *Alu* sequences that were differentially active during primate evolution, as well as an *Alu* RNA sequence that is currently active in humans. Mutations that accompanied *Alu* RNA evolution led to changes in a conserved structural motif also found in SRP RNAs that are associated with thermodynamic destabilization and decreased affinity of the *Alu* right monomer for SRP9/14. In contrast to the right monomer, the *Alu* left monomer maintained structural integrity and high affinity for SRP9/14, indicating that sc*Alu* RNA has been under selection during human evolution. Loss of *Alu* right monomer affinity for SRP9/14 is associated with sc*Alu* RNA production from *Alu* elements in vivo. Moreover, the loss in affinity coincided with decreased rates of *Alu* amplification during primate evolution. This indicates that stability of the *Alu* right monomer is a critical determinant of *Alu* retroposition. These results provide insight into *Alu* mobility and evolution and into how retroposons may interact with host proteins during genome evolution.**

At nearly 1 million copies in primate DNA, *Alu* interspersed elements are the most successful transposons known. The great majority of *Alu* repeats in human DNA were fixed in an ancestral primate genome before the emergence of the human lineage (reviewed in reference 40). Although *Alu* retroposition indeed occurs in humans (16, 35, 46, 48), the available data indicate that (i) certain *Alu* sequences have been more prolific than others and (ii) the rate of new *Alu* insertions into the genome has declined during recent periods of primate evolution (6, 40, 41).

The *Alu* retroposons that were actively proliferating during ancient, intermediate, and modern evolutionary times are reflected by three subfamilies of *Alu* sequences that remain distinguishable in human DNA (7, 23, 38, 44, 50; reviewed in references 40 and 41). The subfamily consensus sequence referred to as *Alu* Sx (formerly PS and Major; see nomenclature in reference 2) represents the sequence that produced approximately 85% of the *Alu*s in the human genome 60 to 30 million years ago. The *Alu* Y sequence (formerly CS and Precise) was active 30 to 15 million years ago and represents ~15% of *Alu* sequences in human DNA. The *Alu* Ya5 consensus (formerly HS and PV) represents the sequence that was active over the last 5 million years that produced <0.5% of the *Alu* sequences in human DNA (2, 3, 14, 22, 27, 33, 38, 40, 41). These data argue that the average *Alu* retroposition rate in the human lineage has been only 1% that in early primates (13).

Structural evidence indicates that *Alu* transcripts synthesized by RNA polymerase (Pol) III are subsequently copied 3′ to 5′ (3′→5′) into cDNA as part of the retroposition process (reviewed in reference 40). *Alu* retroposition is therefore probably governed by the rate of *Alu* transcription, stability of the RNA product, and the rate of cDNA synthesis, and all else being equal, changes in either of these parameters would be expected to influence the *Alu* retroposition rate. The present study is concerned with the second parameter, stability of the *Alu* transcript, and how this is affected by the *Alu* RNA binding protein, SRP9/14. The *Alu* element is dimeric, composed of a 5′ left monomer and a 3′ right monomer that differ in size and sequence. In cells, Pol III-synthesized *Alu* transcripts exist in two forms, heterogeneous dimeric RNAs that contain A-rich tracts and variable 3′ ends and a more homogeneous group of shorter transcripts known as small cytoplasmic *Alu* (sc*Alu*) RNA that corresponds precisely to the *Alu* left monomer (8, 28, 29, 31, 34). Dimeric *Alu* RNAs (hereafter referred to as full-length or fl*Alu*) are labile, giving rise to long-lived sc*Alu* RNA by RNA 3′-end processing (12, 31). Since only fl*Alu*s constitute active retroposons, sc*Alu* RNA production represents a way to decrease the propensity for *Alu* mobility by decreasing the amount of fl*Alu* RNA available for retroposition. Certain conditions cause fl*Alu* RNA levels to increase disproportionately to sc*Alu* RNA, suggesting a physiologic function for *Alu* RNA and a link between cell stress and retroposition (28, 36). An independent function for sc*Alu* RNA is suggested by its accumulation as a stable ribonucleoprotein (RNP) that is partitioned to the cytoplasm (8). Thus, interest in *Alu* has focused on two issues, evolutionary aspects of *Alu* retroposition and cellular function (5, 9–12, 28, 29, 34).

Alu sequences were ancestrally derived from the 5′ and 3′ terminal regions of the 7SL RNA component of the signal recognition particle (SRP) (reviewed in reference 21). These regions in 7SL RNA base pair to form a specific cruciform structure that is recognized by the heterodimeric SRP protein

* Corresponding author. Mailing address: Laboratory of Molecular Growth Regulation, National Institute of Child Health and Human Development, National Institutes of Health, Building 6, Room 416, 9000 Rockville Pike, Bethesda, MD 20892-2753. Phone: (301) 402-3567. Fax: (301) 480-9354. E-mail: maraia@ncbi.nlm.nih.gov.

known as SRP9/14 (18, 49). This structure is grossly conserved in consensus fl*Alu* RNAs, and it has been shown that cellular sc*Alu* transcripts associate with SRP9/14 (5, 10, 25, 31, 42). Conservation of the *Alu* cruciform structure by fl*Alu* consensuses suggests that interaction with SRP9/14 has had a positive effect on *Alu* retroposition, presumably at the level of RNA stability. A role for SRP9/14 in *Alu* mobility is also suggested by the fact that in humans and modern primates SRP9/14 levels are 10- to 20-fold higher than 7SL RNA levels (5, 11). This deregulation is associated with genetic polymorphisms in SRP14 and occurred during the primate evolutionary period that witnessed the greatest burst of *Alu* amplification known (11). Moreover, coincidences between structural changes in SRP9/14 and calculated rates of *Alu* amplification strengthen the contention that *Alu* amplification was modulated by adaptations in SRP9/14 (11, 32). As discussed above, the *Alu* sequence itself changed during primate evolution, and although this might have affected its interaction with SRP9/14, a way to test this had been lacking.

For the present study we constructed consensus sequences representing the *Alu* elements that were differentially active during primate evolution and used them to produce monomeric and fl*Alu* RNAs in vitro and in vivo. The ability of these RNAs to interact with SRP9/14 in vitro and to generate sc*Alu* RNA in vivo was examined. Changes in overall RNA structure, including SRP9/14 binding sites, occurred in the right monomer of the human *Alu* retroposon. Progressive diminution in the affinity between the *Alu* right monomer and SRP9/14 occurred as the *Alu* sequence evolved in higher primates. This was accompanied by an increased propensity for sc*Alu* RNA production, presumably due to loss of SRP9/14 binding by the 3′ monomer, and a decline in the *Alu* retroposition rate.

MATERIALS AND METHODS

***Alu* consensus DNA templates.** The synthetic consensus sequence *Alu* K developed by Kariya et al. and modified by Vorce et al. to *Alu* V (24, 39, 47) was converted to a PS *Alu* (41) by PCR-mediated mutagenesis using appropriate primers by a method described previously (8). The PS consensus sequence contains only one mismatch to the Sx consensus, since G occupies position 163 in PS (as it does in *Alu* Y, Ya5, and the corresponding residue in 7SL RNA) (2, 4, 41). For the sake of simplicity we will refer to this consensus as Sx. The *Alu* repeat within the fourth intron of the human AFP gene was converted to *Alu* Y by PCR-directed mutagenesis (17). *Alu* Ya5 was from pPD39 (provided by M. Batzer, Louisiana State University, New Orleans), a perfect match to its consensus (1). Due to technical limitations, the constructs for the Sx and Y dimeric sequences carried one and four substitutions, respectively: $G_{81}\rightarrow A$ in Sx and $C_{100}\rightarrow T$, $G_{147}\rightarrow A$, $C_{151}\rightarrow T$, and $G_{208}\rightarrow T$ in Y; numbering is according to reference 2. Nevertheless, the Sx dimeric sequence used here is >99% identical to the Sx consensus, and the dimeric Y sequence is >98% identical to *Alu* Y (2, 13). All the monomeric RNAs used in this study are identical to their consensuses.

RNA EMSA. For in vitro RNA synthesis, promoters for T7 RNA polymerase were positioned by PCR to initiate RNA synthesis at the first base of the *Alu* sequence and to terminate at the last base of the *Alu* sequence as described previously (30). *Alu* monomer electrophoretic mobility shift assays (EMSAs) were performed with SRP9/14 that was purified from HeLa cells (heparin agarose fraction) (10). *Alu* dimer EMSAs were performed with cytoplasmic extract of owl monkey cells as described previously (11, 19). RNAs were synthesized in parallel reactions using a common pool of nucleoside triphosphates and [α-^{32}P]GTP to ensure [^{32}P]RNA products of the same specific activity. Nonradioactive, specific RNA competitors were synthesized without [α-^{32}P]GTP. All RNAs were gel purified before use and the integrity of each was confirmed by gel electrophoresis. Nonradioactive RNAs were quantitated by denaturing polyacrylamide gel electrophoresis (PAGE)-ethidium staining and densitometry by using NIH Image version 154 beta software (from W. Rasband, National Institute of Mental Health, National Institutes of Health). Quantitation of EMSA results was by a PhosphorImager using ImageQuant software (Molecular Dynamics).

Transfection. The *Alu* dimer consensus sequences were modified by attaching the sequence AAAAGGCTTTT to their 3′ end, providing a short A-rich tail and a Pol III terminator. The resulting *Alu* DNAs were cloned into the *Hin*dIII/*Eco*RI sites of pUC18 (Bethesda Research Laboratories) and designated p*Alu*-PS (Sx), p*Alu*-CS (Y), and p*Alu*-HS (Ya5). Transfection was carried out as described previously (10). RNA purification and denaturing PAGE were as described previously (30) except that the DNase I treatment was for 2 h, as we found this necessary to fully clear the transfected plasmid. Northern (RNA) blot analysis was with ^{32}P-, end-labelled oligonucleotide DNA probes complementary to residues 67 to 90 (*Alu* left) and residues 213 to 236 (*Alu* right; numbering according to reference 2). Each probe was redundant at the appropriate positions to accommodate *Alu* Sx, Y, and Ya5 sequences and was used as described previously (8).

RESULTS

Efficient binding of SRP9/14 to *Alu* left monomer transcripts. The RNA EMSA was recently used to demonstrate that SRP9/14 recognizes 7SL and sc*Alu* RNAs with similar affinity (K_d of 0.2 and 0.3 nM, respectively) (19). Figure 1 shows EMSAs of binding between SRP9/14 and left monomer consensus [^{32}P]RNAs compared in parallel. Left monomer RNAs derived from Sx, Y, and Ya5 consensuses each formed an RNP complex with SRP9/14 with only modest differences in binding efficiency (Fig. 1A). Left monomer RNA derived from *Alu* Sx (lane 2) exhibited the least efficient binding, while *Alu* Y (lane 4) and Ya5 (lane 6) were about three- and twofold higher, respectively. EMSAs performed over a range of SRP9/14 concentrations (0.15 to 1.2 nM) confirmed these differences (Fig. 1B). Each of the RNAs exhibited substantial binding below 1 nM SRP9/14, consistent with previous findings for an *Alu* left monomer RNA derived from a natural *Alu* Ya5 element (19).

The data in Fig. 1A and B indicate that the left monomers of active *Alu* retroposons as represented by these consensus sequences have changed little in their ability to interact with SRP9/14. Ancestral relatedness, similar predicted and determined structures, and similar SRP9/14 binding coefficients provide reasonable certainty that SRP9/14 binds to *Alu* RNAs in the same manner as it binds to 7SL RNA (19, 42) (see reference 30 and references therein). SRP9/14 binds to a cruciform structure formed by the first 65 and last 15 nucleotides (nt) of 7SL RNA (45). Left monomers of *Alu* Sx, Y, and Ya5 consensus sequences can be folded into structures that are nearly identical to 7SL RNA in this region (25, 26) (Fig. 1C). The consensuses for the *Alu* left monomers are 100% identical for the first 64 nt, are divergent from nt 65 to 100, and are identical again from nt 101 to 116. The *Alu* left monomer RNA depicted in Fig. 1C corresponds to the Sx sequence. Regions corresponding to all the 7SL RNA SRP9/14 binding sites determined by Strub et al. (45) are conserved in the *Alu* left monomer RNA (not shown). For the sake of brevity and reference in a later section, three SRP9/14 binding sites are designated IB, IIB, and IV (45); these are indicated on the *Alu* left monomer RNA (Fig. 1C).

The sc*Alu* RNA exhibits a cruciform domain that is highly conserved through higher primate evolution and contains all known binding sites for SRP9/14 and a divergent domain that contains no known binding sites for SRP9/14 (Fig. 1C). It may be significant that deletion of dinucleotide $C_{65}U_{66}$ and substitution of U_{100} occurred just beyond, yet very close to, SRP9/14 binding site IV, as the *Alu* left monomer evolved from the Sx to the Y sequence. These differences may be responsible for the subtle effects on SRP9/14 binding described above.

Alterations occurred in the structure of *Alu* right monomer transcripts. Native gel electrophoresis is a valuable tool for detecting differences in RNA structure (15). In contrast to the left monomer RNAs, the right monomer RNAs migrated with distinct electrophoretic mobilities on native gels. Right monomer RNAs were examined after electrophoresis on a native polyacrylamide gel, excised, purified, and reexamined on a denaturing polyacrylamide gel that contained 8 M urea (Fig. 2A, left and right panels, respectively). The Sx right monomer

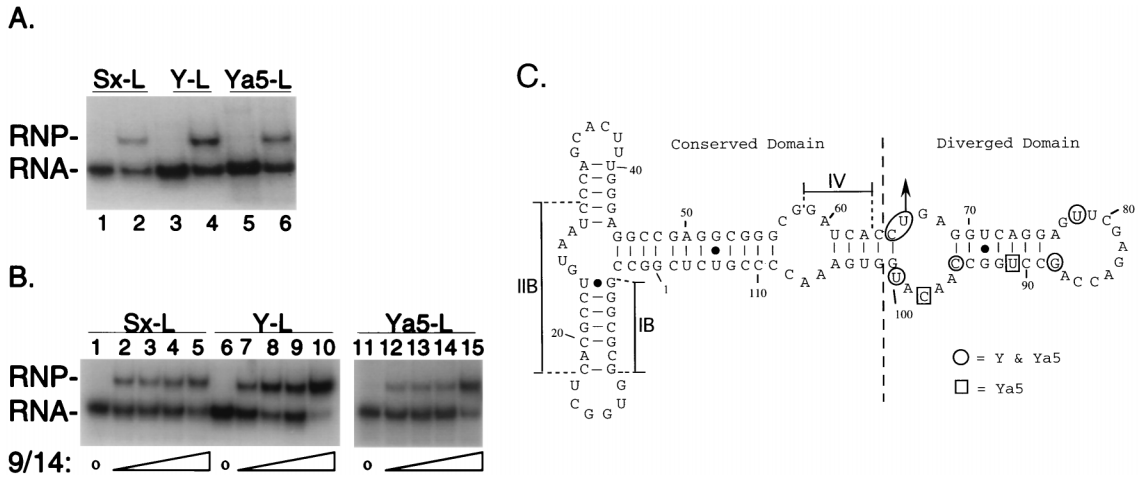

FIG. 1. SRP9/14 binds to *Alu* Sx, Y, and Ya5 left monomer RNAs with similar efficiencies. (A) ^{32}P-labelled, gel-purified left monomer RNAs (0.1 ng) of Sx, Y, and Ya5 subfamily consensus sequences incubated for 30 min in EMSA buffer alone (lanes 1, 3, and 5) or buffer containing 0.2 ng of purified SRP9/14 (lanes 2, 4, and 6). Products were electrophoresed on 6% native polyacrylamide gels, dried, and exposed to X-ray film. Positions of free RNA and RNP complexes are indicated on the left. (B) ^{32}P-labelled, gel-purified left monomer RNAs (0.1 ng) of Sx, Y, and Ya5 subfamily consensus sequences incubated for 30 min in EMSA buffer alone (lanes 1, 6, and 7) or buffer containing increasing amounts of purified SRP9/14, as follows: lanes 2, 7, and 12, 0.05 ng; lanes 3, 8, and 13, 0.1 ng; lanes 4, 9, and 14, 0.2 ng; lanes 5, 10, and 15, 0.4 ng. (C) Predicted secondary structure of *Alu* left monomer RNA based on the phylogenetically conserved *Alu* domain structure and minimal free energy calculations (26, 51). Although the structure predicted did not include a base pair between G11 and C18, it was included here because this is a phylogenetically conserved base pair even when the residues proximal to it are unpaired (26). Nucleotide changes that accompanied *Alu* subfamily evolution are shown in circles for Y and Ya5 and in boxes for Ya5 only, as indicated. The dinucleotide $C_{65}U_{66}$ is absent in Y and Ya5; nucleotides at other positions are A_{78}, U_{88}, C_{91}, U_{95}, A_{98}, and C_{100}. SRP9/14 binding sites designated IB, IIB, and IV are indicated (see text) (45). A dashed vertical line dissects the RNA structure into a conserved domain that is invariant in sequence among the Sx, Y, and Ya5 consensuses and a diverged domain as indicated (see text).

migrated differently from the Y and Ya5 right monomers under native conditions (left panel), while they all migrated with the same mobility in denaturing gels (right panel). Thus, even though Sx and Y right monomer RNAs are identical in length and differ only at four positions, they adopt different structures.

Mutations in multiple SRP9/14 binding sites accumulated in the right monomers of modern *Alu* retroposons. RNA structure predictions suggested that the Sx right monomer was more compact than *Alu* Y and Ya5 right monomers, consistent with their relative mobilities in native gels. Figure 2B compares the predicted structures for the Sx and Y right monomer RNAs

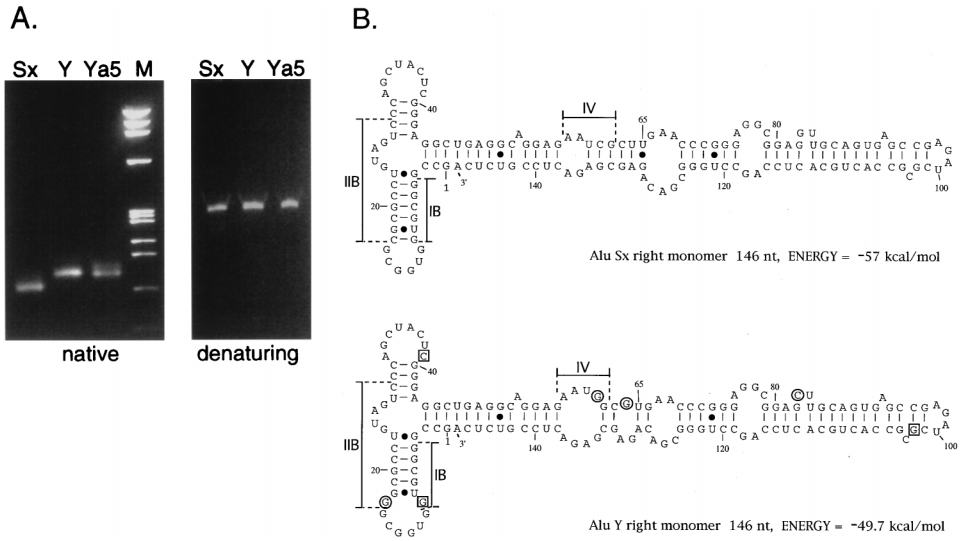

FIG. 2. Consensus *Alu* right monomer RNAs adopt different structures and exhibit progressive mutations in their SRP9/14 binding sites. (A) Comparison of *Alu* right monomer RNAs by PAGE. One hundred nanograms of each right monomer RNA was suspended in Tris-EDTA buffer lacking Mg^{2+} and electrophoresed on a 6% native polyacrylamide gel (left panel). The RNAs were excised from the native gel, eluted, precipitated, resuspended in 98% formamide lacking Mg^{2+}, and electrophoresed on a 6% polyacrylamide gel containing 8 M urea (right panel). After electrophoresis, gels were stained with ethidium bromide, destained, transilluminated with UV light, and photographed. Lane M reveals a *Hae*III digest of ϕX174. (B) Sequences and predicted secondary structures of the *Alu* Sx (upper) and *Alu* Y (lower) right monomer RNAs based on the phylogenetically conserved *Alu* domain structure and minimal free energy calculations (26, 51). The *Alu* Y structure highlights the substitutions relative to Sx with circles (see upper panel for nucleotide identities). The *Alu* Y residues G10, C39, and G102 are highlighted in boxes to indicate that these are substituted in *Alu* Ya5: these are A, U, and C, respectively, in Ya5. SRP9/14 binding sites designated IB, IIB, and IV are indicated (see text).

(Ya5 is superimposed on Y for brevity). Calculated minimal free energies for Sx, Y, and Ya5 right monomers are −57, −49.7, and −48.6 kcal/mol, respectively (20, 51). A minimal free energy difference of 13% between the Sx and Y right monomer secondary structures is remarkable, since these are less than 3% divergent in sequence. From this relatively large energy difference we presume for the purposes of this study that these structures reflect the stable conformers observed by native gel electrophoresis in Fig. 2A. The significance of the structural differences is analyzed below.

We examined the sequences corresponding to SRP9/14 binding sites in *Alu* right monomers. In Sx, Y, and Ya5 right monomers, the first 65 and last 17 nt form the *Alu* cruciform structure and share 93, 89, and 87% identity with corresponding sequences in 7SL RNA, respectively (not shown). Notable differences among these *Alu* sequences occur on both sides of the hairpin structure that encompasses nt 4 to 23 and in the region containing nt 58 through 65 of the upper strand of the RNAs, as compared in Fig. 2B. These differences correspond to nucleotides within SRP9/14 binding sites IB, IIB, and IV, respectively (45).

Binding site IV corresponds to residues 58 to 62, as designated by Strub et al. (45). *Alu* Sx differs from *Alu* Y and Ya5 by a single nucleotide substitution in SRP9/14 binding site IV, namely, C_{61}→G. This single substitution led to disruption of two base pairs in the predicted region of *Alu*s Y and Ya5 (Fig. 2B, lower panel). To gain insight into the potential significance of this observation we examined predicted structural characteristics of the five nt that compose binding site IV in eukaryotic SRP RNAs. This was facilitated by the SRP RNA sequence compilation of Larsen and Zwieb (26). These authors assigned secondary structure characteristics (i.e., paired or unpaired) to each nucleotide in the aligned sequences. In the SRP RNAs from *Caenorhabditis elegans* to humans as well as in plants, the first 2 nt of the pentameric site IV sequences are predicted to lie in an internal loop, and the following 3 nt are involved in highly conserved base pairs (26). This suggests that the paired-versus-unpaired nature of each of these residues is important for SRP9/14 recognition. These characteristics are also maintained in the *Alu* Sx right monomer RNA (Fig. 2B, upper panel), while mutations in *Alu* Y and Ya5 right monomer RNAs have disrupted two of the three base pairs in this structural motif (Fig. 2B, lower panel).

Binding site IIB contains one of the most highly conserved sequence tracts in SRP RNAs and is in part base paired with binding site IB residues to form a highly conserved hairpin structure, as indicated in Fig. 2B (45). It was previously shown that the site IB and IIB residues G_{10} and C_{17} form a highly conserved base pair in higher eukaryotic SRP RNAs and that both of these residues are in close contact with SRP9/14 in human 7SL RNA (26, 45). The *Alu* Sx right monomer preserves the G_{10}:C_{17} base pair, while the *Alu* Y and Ya5 right monomer RNAs do not (Fig. 2B). C_{17} is substituted in *Alu*s Y and Ya5, and G_{10} is further substituted in Ya5. Thus, the *Alu* Ya5 right monomer contains the double mutation A_{10} G_{17} in place of the base pair G_{10}:C_{17}. These observations suggested that alterations of binding sites IB, IIB, and IV in *Alu* Y and Ya5 right monomer RNAs might be associated with decreased affinity for SRP9/14 compared to the Sx right monomer. This was demonstrated as described below.

SRP9/14 exhibits differential binding to consensus *Alu* right monomer RNAs. In contrast to modest binding differences observed for *Alu* left monomers, *Alu* right monomer RNAs were quite different in their binding to SRP9/14. EMSAs performed over a range of SRP9/14 concentrations demonstrated a significant difference in binding affinity among the right monomer RNAs (Fig. 3, lanes 1 to 12). Most of the Sx RNA was shifted to the RNP band at low concentrations of SRP9/14, while Y RNA required higher concentrations for efficient RNP formation (compare lanes 2 and 6). Even at high SRP9/14 concentrations a significant fraction of the Y RNA remained unbound (lanes 7 and 8). The Ya5 right monomer [^{32}P]RNA consistently exhibited the lowest affinity for SRP9/14, since most of it remained unbound even at the highest SRP9/14 concentrations tested, with relatively little RNP formation (lanes 10 to 12). The same pattern of relative binding affinity was also observed with specific and nonspecific competitor RNAs; Sx right monomer always interacted most efficiently with SRP9/14, while Ya5 did so least efficiently (not shown). Although we did not determine precise binding coefficients, quantitation of these and other results indicate that the *Alu* Y right monomer exhibits three- to fivefold lower affinity for SRP9/14 than does the *Alu* Sx right monomer, while the *Alu* Ya5 right monomer exhibits 10- to 20-fold lower affinity (19). As a binding calibration reference, *Alu* Ya5 left monomer RNA (Fig. 3, lanes 13 to 16) was compared to the *Alu* right monomer RNAs (lanes 1 to 12) in parallel. This revealed that Ya5 left monomer RNA was similar to Sx right monomer RNA in its affinity for SRP9/14 (compare lanes 13 to 16 with lanes 1 to 4) and that Ya5 left and right monomer RNAs exhibited a significant difference in affinity (compare lanes 9 to 12 with lanes 13 to 16).

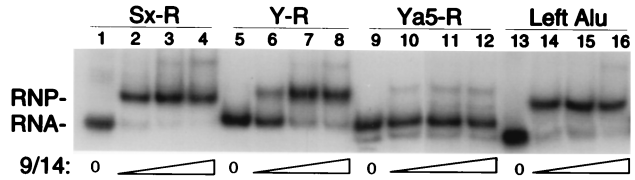

FIG. 3. SRP9/14 binds to consensus *Alu* right monomer RNAs with different efficiencies. ^{32}P-labelled, gel-purified right monomer RNA Sx, Y, and Ya5 subfamily consensus sequences and a Ya5 left monomer [^{32}P]RNA were incubated for 30 min in EMSA buffer alone or buffer containing increasing amounts of highly purified SRP9/14 (10). Reconstitution products were electrophoresed on 6% native polyacrylamide gels, dried, and exposed to X-ray film. Amounts of SRP9/14 included in the reaction mixtures were as follows: lanes 1, 5, 9, and 13, none; lanes 2, 6, 10, and 14, 1 ng; lanes 3, 7, 11, and 15, 2 ng; lanes 4, 8, 12, and 16, 4 ng. Positions of free RNA and RNP are indicated.

SRP9/14 binds to dimeric *Alu* RNAs with high affinity. Although unlikely, it nonetheless seemed possible that consensus fl*Alu* RNAs might bind SRP9/14 inefficiently, perhaps due to intermonomeric interactions that might occlude binding sites. Therefore, we wanted to confirm that *Alu* dimers could bind SRP9/14 efficiently by our EMSA approach. Association between a relatively large fl*Alu* [^{32}P]RNA (94 kDa) and the smaller human SRP9/14 (~25 kDa) produced an RNP that was not readily distinguishable from the unbound [^{32}P]RNA (not shown). To more convincingly demonstrate direct binding we used owl monkey cell extract as a source of SRP9/14, which, being larger, produces a more retarded RNP complex (11). We chose to use conditions in which only one molecule of SRP9/14 would bind to fl*Alu* [^{32}P]RNA. Since only one SRP9/14 heterodimer binds to 7SL RNA and it is approximately the same size as fl*Alu* RNA, it was used here as a control. fl*Alu* Sx [^{32}P]RNA and 7SL [^{32}P]RNA migrated similarly when incubated with a limiting amount of SRP9/14, as expected (Fig. 4 and data not shown). *Alu* Sx [^{32}P]RNA produced the most prominent mobility shift, while *Alu* Y and Ya5 [^{32}P]RNA shifts were less efficient (not shown). We used these conditions to examine relative binding of nonradioactive dimeric *Alu* RNAs by monitoring their ability to compete with 7SL [^{32}P]RNA

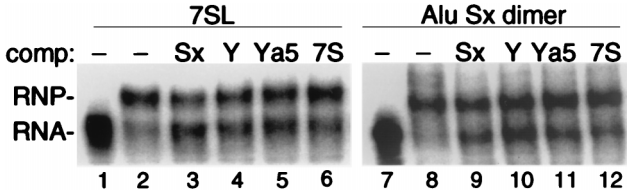

FIG. 4. Full-length *Alu* RNAs bind SRP9/14 with high affinity. EMSA competitions were performed with 0.1 ng of 7SL [^{32}P]RNA (lanes 1 to 6) or fl*Alu* Sx [^{32}P]RNA (lanes 7 to 12) as a probe. Lanes 1 and 7, no added protein; lanes 2 to 6 and 8 to 12, 5 μg of extract derived from owl monkey cells (see text) (11). All reaction mixtures contained 100 ng of poly(G) and 50 ng of poly(U) as nonspecific competitors and either no specific competitor (lanes 2 and 8) or 0.5 ng of the specific full-length competitor indicated above lanes 3 to 6 and 9 to 12.

(Fig. 4, lanes 1 to 6), and Sx fl*Alu* [^{32}P]RNA (lanes 7 to 12) for SRP9/14. Although differences in binding strength were not large, the most effective competitor of 7SL [^{32}P]RNP formation (lanes 1 to 6) was the fl*Alu* Sx. When Sx [^{32}P]RNA was used as a probe (lanes 7 to 12), again the fl*Alu* Sx was a more effective competitor than any other. That fl*Alu* was a better competitor than 7SL RNA was not unexpected, since fl*Alu* exhibits two binding sites for SRP9/14 and its competitive strength is probably a measure of the combined affinities. Experiments using *Alu* left monomer [^{32}P]RNA also demonstrated that fl*Alu* RNAs bound with higher affinity than monomeric *Alu* RNA (not shown). Experiments to compare the binding affinity of the dimeric *Alu* RNAs for a second molecule of SRP9/14 were impeded by technical complications and were inconclusive. Nonetheless, the above experiments indeed demonstrated that as expected, SRP9/14 can interact with consensus fl*Alu* RNAs with high affinity.

Consensus *Alu* retroposons differentially produce sc*Alu* RNA in vivo. We used transfection of NIH 3T3 cells to investigate expression of consensus *Alu* RNAs by Northern blotting. The analysis shown in Fig. 5 was performed on transfected cells that were treated for 0 to 4 h with the transcription inhibitor actinomycin D. The stability of fl*Alu* RNA was similar to what was reported by Chu and coworkers, who examined Ya5 *Alu* RNA in transfected primate cells (12). These consensus *Alu*s reproducibly generated fl*Alu* RNAs whose half lives did not differ when controlled for loading differences with endogenous 5S rRNA (not shown). This analysis is nonetheless useful because it reproducibly demonstrated that although the consensus DNAs indeed generated fl*Alu* RNAs as expected, they produced sc*Alu* RNA with different efficacies (Fig. 5). The *Alu* Ya5 consensus efficiently produced sc*Alu*, while *Alu* Sx and *Alu* Y produced little if any sc*Alu* RNA. This blot was rehybridized with a probe complementary to scB1 RNA, an sc*Alu*-homologous transcript that is endogenous to rodent cells. This revealed scB1 RNA expression in all samples, with no appreciable difference among Ya5-, Y-, and Sx-transfected cells (data not shown).

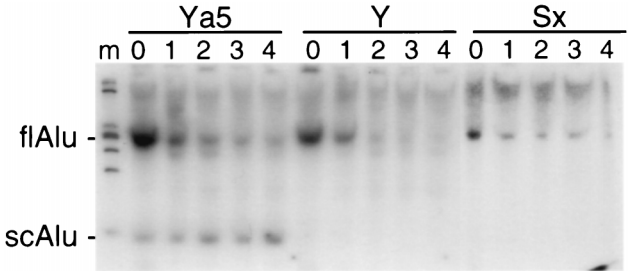

FIG. 5. Northern blot analysis of differential *Alu* RNA metabolism in transfected cells. Twenty-four hours after NIH 3T3 cells were transfected with *Alu* Ya5, Y, and Sx consensus DNA, the cells were treated with actinomycin D for the times indicated above the lanes (in hours). Total RNA was then prepared, coelectrophoresed, transferred to a nylon membrane, and probed with oligonucleotide DNA complementary to the *Alu* left monomers. Positions of fl*Alu* and sc*Alu* RNAs are indicated on the left.

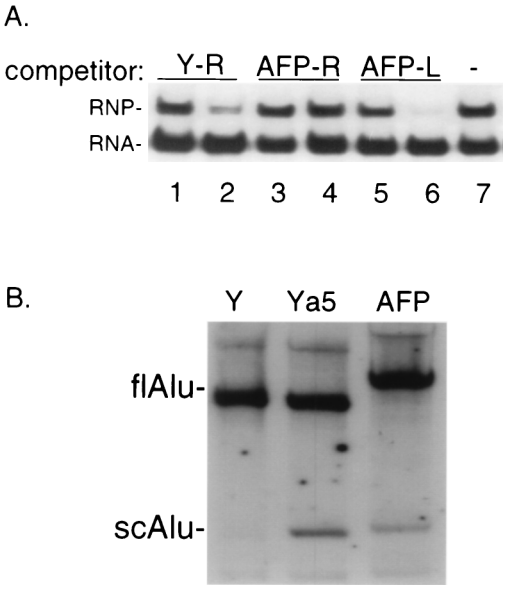

FIG. 6. Low-affinity *Alu* right monomer RNA-SRP9/14 interaction in vitro is correlated with sc*Alu* RNA production in vivo. (A) EMSA competition. Left monomer-derived sc*Alu* [^{32}P]RNA was incubated with SRP9/14 and the following nonradioactive RNA competitors: *Alu* Y right monomer (lanes 1 and 2), AFP-*Alu* right monomer (lanes 3 and 4), and AFP-*Alu* left monomer (lanes 5 and 6). Reaction mixtures in even-numbered and odd-numbered lanes contained 2-fold and 20-fold excesses of nonradioactive RNA, respectively. No competitor RNA was added to the reaction mixture in lane 7. (B) Northern blot analysis of RNA after transfection with *Alu* Y (lane 1), *Alu* Ya5 (lane 2), and AFP-*Alu* (lane 3). RNA was purified 24 h after transfection, coelectrophoresed, transferred to a nylon membrane, and probed with oligonucleotide DNA complementary to a region in the *Alu* left monomer. Note that this AFP-*Alu* produces an fl*Alu* transcript that is longer than the consensus DNAs because its terminator is located in downstream DNA (31).

One explanation to account for the pattern of sc*Alu* RNA observed is that sc*Alu* RNA expression is determined by the sequence of the Ya5 left monomer. However, sc*Alu* RNA is produced in vivo by members of all three *Alu* subfamilies (31). Therefore, an alternative explanation is that the propensity to produce sc*Alu* RNA is determined by a difference in affinity between the *Alu* right and left monomers, such that a low-affinity right monomer promotes sc*Alu* RNA production (see Discussion). An experiment designed to discriminate between the above possibilities is presented in Fig. 6. A naturally occurring *Alu*, derived from the fourth intron of the human alphafetoprotein (AFP) gene, has previously been assigned to the *Alu* Y subfamily and contains several random mutations in comparison to the Y consensus (40). However, unlike other *Alu* Y subfamily members, AFP-*Alu* is human specific and is therefore atypical of *Alu* Y subfamily members (see Discussion). Figure 6 shows that the right monomer RNA from AFP-*Alu* exhibits a much reduced affinity for SRP9/14 compared to its left monomer, as demonstrated by low competitive strength in the EMSA. AFP-*Alu* right monomer RNA (lanes 3 and 4) competed for SRP9/14 less efficiently than did *Alu* Y right monomer RNA (lanes 1 and 2), while AFP-*Alu* left monomer RNA competed much better, as expected (lanes 5 and 6).

Next, we examined the ability of AFP-*Alu* to generate sc*Alu*

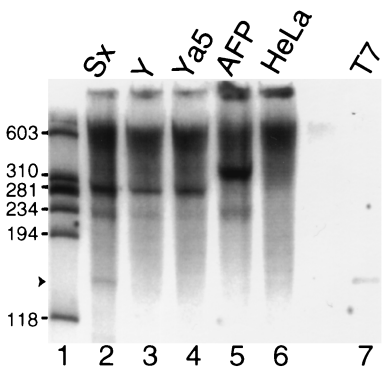

FIG. 7. *Alu* Sx but not *Alu* Y or Ya5 right monomer RNA accumulates in vivo. Shown is a northern blot analysis of HeLa cell RNA and RNA isolated from NIH 3T3 cells after transfection with *Alu* Sx, Y, Ya5, and AFP-*Alu* DNAs as indicated above lanes 2 to 6. Lane 7 contained 0.5 pg of a nonradioactive, 147-nt RNA synthesized in vitro from an *Alu* right monomer, used here as a control. Lane 1 contained a *Hae*III digest of ϕX174 denatured [^{32}P]DNA; sizes of marker bands are indicated on the left in nucleotides. The probe is complementary to the *Alu* right monomer. Arrowhead at left indicates the position of 147-nt Alu right monomer RNA.

RNA. AFP-*Alu* was transfected in parallel with *Alu*s Y and Ya5, and RNA expression was monitored by Northern blot analysis (Fig. 6B). The AFP-*Alu* produces an fl*Alu* transcript that is longer than the consensus DNAs because its terminator is located farther downstream (31). Nevertheless, AFP-*Alu* and *Alu* Ya5 generated sc*Alu* RNA, while *Alu* Y did not. In addition to confirming that left monomers other than Ya5 can produce sc*Alu* RNA, these results strengthen the hypothesis that sc*Alu* RNA accumulation is correlated with a low affinity site in the right monomer.

Finally, we examined RNA from transfected cells using a probe specific for *Alu* Sx, Y, and Ya5 right monomers (Fig. 7). This probe detected dimeric *Alu* RNA in all of the transfected samples, as expected (lanes 2 to 5). A nonradioactive 147-nt synthetic AFP-*Alu* right monomer RNA (used in Fig. 6A) was used here as a positive control (lane 7). An ~147-nt RNA was also detectable after transfection with *Alu* Sx (arrowhead, lane 2) but not with *Alu* Y, Ya5, or AFP-*Alu* or in HeLa cell RNA (lanes 3 to 5, respectively). Although we have not mapped the termini of the cellular ~147-nt transcript produced by *Alu* Sx DNA, its size suggests that it represents a discrete *Alu* right monomer. Accumulation of this RNA specifically in *Alu* Sx-transfected cells is consistent with its affinity for SRP9/14, which is significantly higher than those of *Alu* Y, Ya5, and AFP-*Alu* right monomers. The important result here is that in cells transfected with *Alu* Ya5 and AFP-*Alu*, and in HeLa cells, left monomer RNA accumulates while right monomer RNA does not. Thus, although the accumulation of *Alu* Sx right monomer RNA is somewhat artificial here, since right monomers do not accumulate in HeLa cells, these data support the binding results obtained in vitro and suggest that *Alu* RNA metabolism in vivo is determined in part by the ability of *Alu* sequence RNA to interact with SRP9/14.

DISCUSSION

In this study we have tried to explain how nucleotide changes in the *Alu* sequence may have affected *Alu* retroposon activity. Sequence transitions from *Alu* Sx→Y→Ya5, which were accompanied by declines in *Alu* amplification rates, were associated with a significant decrease in the ability of the *Alu* right monomer to interact with SRP9/14. This was due to alterations of SRP9/14 binding sites in the *Alu* right monomer as the *Alu* sequence evolved in higher primate and human lineages. Alterations in Alu RNA metabolism as the *Alu* sequence evolved from *Alu* Y→Ya5 were suggested by an increase in the propensity for sc*Alu* RNA production. Binding of SRP9/14 to the right monomer may protect *Alu* RNA from 3′ processing, thereby allowing the RNA to be copied 3′→5′ by reverse transcriptase. The *Alu* Ya5 retroposon sequence exhibits the lowest right monomer affinity for SRP9/14, is the most proficient at sc*Alu* RNA production, and, as discussed in the introduction, appears to be the least successful at retroposition. From these observations we speculate that *Alu* RNA 3′ processing was a significant factor in controlling *Alu* retroposition in the human genome.

Asymmetry of SRP9/14 binding sites in fl*Alu* RNA leads to sc*Alu* RNA. We propose that any dimeric *Alu* transcript would be susceptible to sc*Alu* RNA production if its right monomer lacks the ability to interact efficiently with SRP9/14, provided that the left monomer retains efficient binding. The heterogeneity in cellular *Alu* RNAs that is generated by sequence drift suggests that some transcripts from any subfamily would fulfill these criteria (29, 31, 43). Therefore, we wish to emphasize that sc*Alu* RNA production in cells is not limited to *Alu* Ya5 sequences. That the relative affinity between the left and right monomers of an individual *Alu* dimeric transcript may determine the propensity for sc*Alu* RNA expression was demonstrated in Fig. 6: consensus *Alu* Y does not produce sc*Alu* RNA, while AFP-*Alu*, an *Alu* Y member that contains six random substitutions in its right monomer and a demonstrably low affinity for SRP9/14, does. It is intriguing that although AFP-*Alu* has been assigned to the Y subfamily by sequence comparison, it better resembles *Alu* Ya5 in that (i) it is human specific, having transposed within the last 5 million years, (ii) it produces sc*Alu* RNA, and (iii) its right monomer exhibits low affinity for SRP9/14.

The fact that the AFP-*Alu* right monomer exhibits low affinity for SRP9/14 while its left monomer exhibits high affinity provides evidence to suggest that SRP9/14 binding is more sensitive to sequence drift in the *Alu* right monomer RNA than in the left monomer, although the reason for this is unclear. Nonetheless, this asymmetry appears to have led to an increasing propensity for sc*Alu* RNA production during primate evolution. Therefore, this characteristic of the *Alu* sequence exhibited in the AFP-*Alu* repeat appears to reflect sequence drift in the *Alu* retroposon (27).

Although the *Alu* Y and Ya5 right monomers exhibit three nucleotide differences, only two of these are in the *Alu* cruciform structure, yet these monomers exhibit a significant difference in SRP9/14 binding. Although the reason for this is unclear, this result should not be unexpected. One obvious explanation might be that the G_{10} nucleotide contributes a substantial amount of binding energy. This nucleotide is conserved in all mammalian species and is in close contact with SRP9/14 (26, 45). Presumably, loss of binding strength between this nucleotide and SRP9/14 may lead to $N_{18} \cdot U_9$ unpairing and destabilization of the hairpin. Although the effect of the substitution at position 39 is unknown, it was previously shown that substitutions in this loop abrogated binding to SRP9/14 (8).

Structural characteristics of SRP9/14 binding site IV of SRP RNA. During the course of this work evidence which indicates that the precise structure of SRP9/14 binding site IV is important for binding to SRP9/14 was uncovered. This conclusion is based on the highly conserved nature of the secondary structure characteristics of this site in SRP RNAs and the fact that single nucleotide changes in this region were associated with

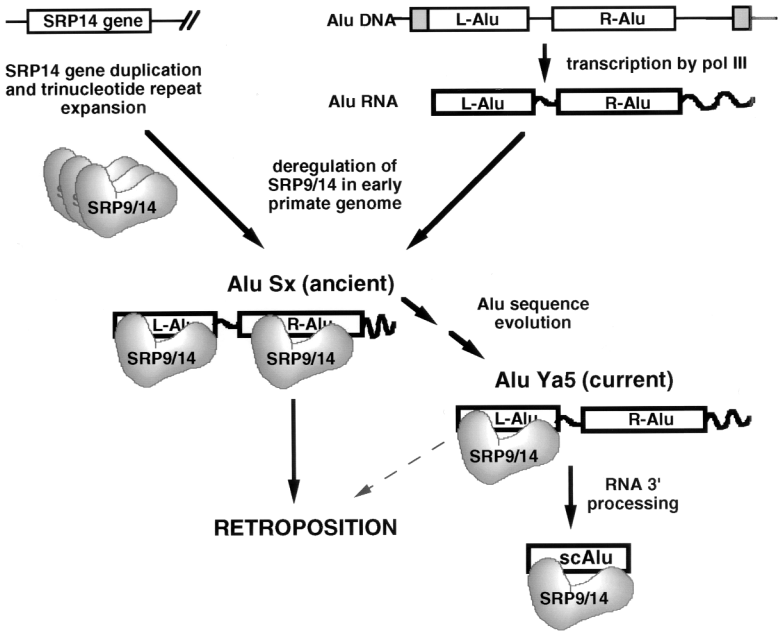

FIG. 8. Model of *Alu* amplification and RNA metabolism in primates. Ancient *Alu* retroposition was initially favored by deregulation of SRP9/14 in early primates (11). Subsequently, *Alu* sequence evolution (subfamily drift) from Sx to Ya5 was associated with decreased binding of SRP9/14 to the right monomer, thereby resulting in decreased *Alu* retroposition. The dashed diagonal line with an arrowhead indicates that *Alu* Ya5 sequences continue to undergo retroposition, albeit at a decreased rate relative to *Alu* Sx, which was a highly successful retroposon. In contrast to the right monomer, the left monomer sequence has been conserved for SRP9/14 binding and sc*Alu* RNA expression. *Alu* Sx also can generate sc*Alu* RNA if sequence drift impairs SRP9/14 binding to the right monomer (not indicated here, but see reference 31 and text for discussion).

significant changes in predicted structure and minimal free energy. Although additional mutations occurred elsewhere in the *Alu* right monomer as the sequence evolved from Sx to Y, we suspect that changes in binding site IV had a substantial effect on affinity for SRP9/14. The effects of site-directed mutations in this region on SRP9/14 binding are consistent with this conclusion (unpublished observation). These results provide insight into the importance of the structure of this site in SRP9/14 binding.

Genetic selection for sc*Alu* RNA. *Alu* Sx→Y→Ya5 sequence changes occurred throughout the right monomer, including in three SRP9/14 binding sites. This is in marked contrast to the situation in the left monomer. Homogeneity of consensus left monomers is also reflected in similar affinities for SRP9/14. Exclusion of sequence changes in the *Alu* cruciform domain of the left monomer but not the right monomer suggests that this was not by chance. Conservation of left monomer binding sites was further revealed by the observation that Sx→Y→Ya5 sequence evolution was limited, even within the left monomer, to the divergent domain exclusively, which does not contact SRP9/14 (Fig. 1B). These phylogenetic comparative data suggest that the ability of sc*Alu* RNA to interact with SRP9/14 has been selected during primate evolution. The A-box promoter element (nt 6 to 15) is represented in part by SRP9/14 binding site IB. However, since the consensus A-box promoter can be quite flexible in sequence (37), and since other SRP9/14 binding sites have also been asymmetrically conserved in the left monomer, transcriptional potential alone appears not to account for the apparent selection for the sc*Alu* RNA-SRP9/14 interaction. The apparent selection for sc*Alu* RNA is reflected in the RNAs that accumulate in vivo in present day cells. While right monomer can be seen by transfection of an extinct *Alu* subfamily, *Alu* Sx, no right monomer RNA accumulates in HeLa cells (Fig. 7). This is in contrast to the readily detectable sc*Alu* RNA in HeLa and other cells (8–10, 12, 29, 33).

The *Alu* sequence as a primary determinant of retroposition activity. Models to account for differential activity of *Alu* retroposons have focused on DNA sequences that flank *Alu* source genes. According to one model, new active retroposons have sprouted whenever a newly transposed *Alu* inserted into a genomic environment conducive to subsequent *Alu* retroposon activity (27, 33). *cis*-acting elements associated with retroposon activity have been attributed to DNA sequences that flank the *Alu* element (27, 40). Another model proposes that the *Alu* master retroposon has been active, albeit at decreasing activity with time, at a single locus (or very few loci) throughout primate evolution (41). According to this model, changes in the activity of the *Alu* retroposon would be due to changes in sequence that flanks or resides within the active *Alu* gene or to changes in a *trans*-acting factor. Interaction of *Alu* RNA with a binding protein that is sensitive to subfamily-specific sequences as described here provides the means by which differential *Alu* retroposon activity may be attributable to the *Alu* sequence itself.

Model of *Alu* amplification. From earlier results and those presented here, we are now able to construct a model that can explain the course of *Alu* amplification in primates (Fig. 8). SRP9/14 was deregulated in an early primate genome such that its levels rose 10- to 20-fold higher than its cognate 7SL RNA (5, 11). During the same period the number of *Alu* Sx sequences was greatly expanded in a burst of amplification. As the *Alu* Sx sequence evolved to *Alu* Y and then to *Alu* Ya5, its affinity for SRP9/14 decreased progressively coincident with the *Alu* amplification rate. Thus, in ancient times *Alu* Sx was more prolific because its RNA was stabilized, while in current times *Alu* Ya5 is less prolific. Since these changes were medi-

ated through the *Alu* right monomer, sc*Alu* RNA and its ability to form stable RNP with SRP9/14 remained unaltered.

ACKNOWLEDGMENTS

We are grateful to P. Deininger and M. Batzer for pPD39 and G. Humphrey and R. Vorce for *Alu* V and to A. V. Furano for critical reading and helpful suggestions, to an anonymous referee for suggesting a model figure, and to C. Schmid for comments and discussion.

REFERENCES

1. **Batzer, M. A., M. Alegria-Hartman, and P. L. Deininger.** 1994. A consensus Alu repeat probe for physical mapping. Genet. Anal. Technol. Appl. **11:**34–38.
2. **Batzer, M. A., P. L. Deininger, U. Hellmann-Blumberg, J. Jurka, D. Labuda, C. M. Rubin, C. W. Schmid, E. Zietkiewicz, and E. Zuckerkandl.** 1996. Standardized nomenclature for Alu repeats. J. Mol. Evol. **42:**3–6.
3. **Batzer, M. A., V. A. Gudi, J. C. Mena, D. W. Foltz, R. J. Herrera, and P. L. Deininger.** 1991. Amplification dynamics of human-specific (HS) alu family members. Nucleic Acids Res. **19:**3619–3623.
4. **Batzer, M. A., C. W. Schmid, and P. L. Deininger.** 1993. Evolutionary analyses of repetitive DNA sequences. Methods Enzymol. **224:**213–232.
5. **Bovia, F., M. Fornallaz, H. Leffers, and K. Strub.** 1995. SRP9/14 subunit of the signal recognition particle (SRP) is present in more than 20-fold excess over SRP in primate cells and exists primarily free but also in complex with small cytoplasmic Alu RNAs. Mol. Biol. Cell **6:**471–484.
6. **Britten, R. J.** 1994. Evidence that most human *Alu* sequences were inserted in a process that ceased about 30 million years ago. Proc. Natl. Acad. Sci. USA **91:**6148–6150.
7. **Britten, R. J., W. F. Baron, D. B. Stout, and E. H. Davidson.** 1988. Sources and evolution of human *Alu* repeated sequences. Proc. Natl. Acad. Sci. USA **85:**4770–4774.
8. **Chang, D.-Y., and R. J. Maraia.** 1993. A cellular protein binds B1 and Alu small cytoplasmic RNAs *in vitro*. J. Biol. Chem. **268:**6423–6428.
9. **Chang, D. Y., K. Hsu, and R. J. Maraia.** 1996. Monomeric and dimeric Alu RNAs induced by adenovirus assemble into SRP9/14-containing RNPs in HeLa cells. Nucleic Acids Res. **24:**4165–4170.
10. **Chang, D.-Y., B. Nelson, T. Bilyeu, K. Hsu, G. J. Darlington, and R. J. Maraia.** 1994. A human *Alu* RNA-binding protein whose expression is associated with accumulation of small cytoplasmic *Alu* RNA. Mol. Cell. Biol. **14:**3949–3959.
11. **Chang, D.-Y., N. Sasaki-Tozawa, L. K. Green, and R. J. Maraia.** 1995. A trinucleotide repeat-associated increase in the level of *Alu* RNA-binding protein occurred during the same period as the major *Alu* amplification that accompanied anthropoid evolution. Mol. Cell. Biol. **15:**2109–2116.
12. **Chu, W. M., W. M. Liu, and C. W. Schmid.** 1995. RNA polymerase III promoter and terminator elements affect Alu RNA expression. Nucleic Acids Res. **23:**1750–1757.
13. **Deininger, P. L., and M. A. Batzer.** 1993. Evolution of retroposons. Evol. Biol. **27:**157–196.
14. **Deininger, P. L., M. A. Batzer, C. A. Hutchison III, and M. H. Edgell.** 1992. Master genes in mammalian repetitive DNA amplification. Trends Genet. **8:**307–311.
15. **Duckett, D. R., A. I. Murchie, and D. M. Lilley.** 1995. The global folding of four-way helical junctions in RNA, including that in U1 snRNA. Cell **83:**1027–1036.
16. **Economou-Pachnis, A., and P. N. Tsichlis.** 1985. Insertion of an Alu SINE in the human homologue of the *Mlvi*-2 locus. Nucleic Acids Res. **13:**8379–8387.
17. **Gibbs, P. E. M., R. Zielinski, C. Boyd, and A. Dugaiczyk.** 1987. Structure, polymorphism, and novel repeated DNA elements revealed by a complete sequence of the human α-fetoprotein gene. Biochemistry **26:**1332–1343.
18. **Gundelfinger, E. D., E. Krause, M. Melli, and B. Dobberstein.** 1983. The organization of the 7SL RNA in the signal recognition particle. Nucleic Acids Res. **11:**7363–7374.
19. **Hsu, K., D. Y. Chang, and R. J. Maraia.** 1995. Human signal recognition particle (SRP) Alu-associated protein also binds Alu interspersed repeat sequence RNAs: characterization of human SRP9. J. Biol. Chem. **270:**10179–10186.
20. **Jaeger, J. A., D. H. Turner, and M. Zuker.** 1989. Improved predictions of secondary structures for RNA. Proc. Natl. Acad. Sci. USA **86:**7706–7710.
21. **Jurka, J.** 1995. Origin and evolution of Alu repetitive elements, p. 25–41. *In* R. J. Maraia (ed.), Impact of short interspersed elements (SINEs) on the host genome. R. G. Landes, Austin, Tex.
22. **Jurka, J., and A. Milosavljevic.** 1991. Reconstruction and analysis of human Alu genes. J. Mol. Evol. **32:**105–121.
23. **Jurka, J., and T. Smith.** 1988. A fundamental division in the *Alu* family of repeated sequences. Proc. Natl. Acad. Sci. USA **85:**4775–4778.
24. **Kariya, Y., K. Kato, Y. Hayashizaki, S. Himeno, S. Tarui, and K. Matsubara.** 1987. Revision of consensus sequence of human Alu repeats—a review. Gene **53:**1–10.
25. **Labuda, D., and E. Zietkiewicz.** 1994. Evolution of secondary structure in the family of 7SL-like RNAs. J. Mol. Evol. **39:**506–518.
26. **Larsen, N., and C. Zwieb.** 1991. SRP-RNA sequence alignment and secondary structure. Nucleic Acids Res. **19:**209–215.
27. **Leeflang, E. P., W.-M. Liu, I. N. Chesnokov, and C. W. Schmid.** 1993. Phylogenetic isolation of a human Alu flounder gene: drift to new subfamily identity. J. Mol. Evol. **37:**559–565.
28. **Liu, W.-M., W.-M. Chu, P. V. Choudary, and C. W. Schmid.** 1995. Cell stress and translational inhibitors transiently increase the abundance of mammalian SINE transcripts. Nucleic Acids Res. **23:**1758–1765.
29. **Liu, W.-M., R. J. Maraia, C. M. Rubin, and C. W. Schmid.** 1994. Alu transcripts: cytoplasmic localization and regulation by DNA methylation. Nucleic Acids Res. **22:**1087–1095.
30. **Maraia, R.** 1991. The subset of mouse B1 (*Alu*-equivalent) sequences expressed as small processed cytoplasmic transcripts. Nucleic Acids Res. **19:**5695–5702.
31. **Maraia, R. J., C. Driscoll, T. Bilyeu, K. Hsu, and G. J. Darlington.** 1993. Multiple dispersed loci produce small cytoplasmic *Alu* RNA. Mol. Cell. Biol. **13:**4233–4241.
32. **Maraia, R. J., and J. Sarrowa.** 1995. Alu-family SINE RNA: interacting proteins and pathways of expression, p. 163–196. *In* R. J. Maraia (ed.), Impact of short interspersed elements (SINEs) on the host genome. R. G. Landes, Austin, Tex.
33. **Matera, A. G., U. Hellmann, M. F. Hintz, and C. W. Schmid.** 1990. Recently transposed Alu repeats result from multiple source genes. Nucleic Acids Res. **18:**6019–6023.
34. **Matera, A. G., U. Hellmann, and C. W. Schmid.** 1990. A transpositionally and transcriptionally competent Alu subfamily. Mol. Cell. Biol. **10:**5424–5432.
35. **Muratani, K., T. Hada, Y. Yamamoto, T. Kaneko, Y. Shigeto, T. Ohue, J. Furuyama, and K. Higashino.** 1991. Inactivation of the cholinesterase gene by Alu insertion: possible mechanism for human gene transposition. Proc. Natl. Acad. Sci. USA **88:**11315–11319.
36. **Panning, B., and J. R. Smiley.** 1993. Activation of RNA polymerase III transcription of human *Alu* repetitive elements by adenovirus type 5: requirement for the E1b 58-kilodalton protein and the products of E4 open reading frames 3 and 6. Mol. Cell. Biol. **13:**3231–3244.
37. **Perez-Stable, C., and C.-K. J. Shen.** 1986. Competitive and cooperative functioning of the anterior and posterior promoter elements of an *Alu* family repeat. Mol. Cell. Biol. **6:**2041–2052.
38. **Quentin, Y.** 1988. The Alu family developed through successive waves of fixation closely connected with primate lineage history. J. Mol. Evol. **27:**194–202.
39. **Sakamoto, K., C. M. Fordis, C. D. Corsico, T. H. Howard, and B. H. Howard.** 1991. Modulation of HeLa cell growth by transfected 7SL RNA and Alu gene sequences. J. Biol. Chem. **266:**3031–3038.
40. **Schmid, C., and R. Maraia.** 1992. Transcriptional regulation and transpositional selection of active SINE sequences. Curr. Opin. Genet. Dev. **2:**874–882.
41. **Shen, M. R., M. A. Batzer, and P. L. Deininger.** 1991. Evolution of the master Alu gene(s). J. Mol. Evol. **33:**311–320.
42. **Sinnett, D., C. Richer, J.-M. Deragon, and D. Labuda.** 1991. *Alu* RNA secondary structure consists of two independent 7 SL RNA-like folding units. J. Biol. Chem. **266:**8675–8678.
43. **Sinnett, D., C. Richer, J.-M. Deragon, and D. Labuda.** 1992. Alu RNA transcripts in human embryonal carcinoma cells: model of posttranscriptional selection of master sequences. J. Mol. Biol. **226:**689–706.
44. **Slagel, V., E. Flemington, V. Traina-Dorge, H. Bradshaw, Jr., and P. L. Deininger.** 1987. Clustering and sub-family relationships of the Alu family in the human genome. Mol. Biol. Evol. **4:**19–29.
45. **Strub, K., J. Moss, and P. Walter.** 1991. Binding sites of the 9- and 14-kilodalton heterodimeric protein subunit of the signal recognition particle (SRP) are contained exclusively in the *Alu* domain of SRP RNA and contain a sequence motif that is conserved in evolution. Mol. Cell. Biol. **11:**3949–3959.
46. **Vidaud, D., M. Vidaud, B. R. Bahnak, B. Siguret, J. M. Lavergne, and M. Goossens.** 1989. Hemophilia B due to a de novo insertion of a human-specific Alu subfamily member within the coding region of the factor IX gene. Eur. J. Hum. Genet. **1:**30–36.
47. **Vorce, R. L., B. Lee, and B. H. Howard.** 1994. Methylation- and mutation-dependent stimulation of Alu transcription in vitro. Biochem. Biophys. Res. Commun. **203:**845–851.
48. **Wallace, M. R., L. B. Andersen, A. M. Saulino, P. E. Gregory, T. W. Glover, and F. S. Collins.** 1991. A *de novo Alu* insertion results in neurofibromatosis type 1. Nature **353:**864–866.
49. **Walter, P., and G. Blobel.** 1983. Disassembly and reconstitution of signal recognition particle. Cell **34:**525–533.
50. **Willard, C., H. T. Nguyen, and C. W. Schmid.** 1987. Existence of at least three distinct Alu subfamilies. J. Mol. Evol. **26:**180–186.
51. **Zuker, M.** 1989. On finding all suboptimal foldings of an RNA molecule. Science **244:**48–52.